JMEPEG (2008) 17:746–754
DOI: 10.1007/s11665-008-9211-y

1059-9495/$19.00

Microstructural Characterization of TLPD bonded 6061-SiCp Composite

Joydeep Maity, Tapan K. Pal, and Rabindranath Maiti

(Submitted April 26, 2007; in revised form February 1, 2008)

Microstructural development during transient liquid phase diffusion (TLPD) bonding of extruded aluminum-based metal matrix composite (6061-15 wt.% SiCp) using 50-µm-thick copper interlayer was investigated by optical microscopy, scanning electron microscopy (SEM) together with SEM-based energy dispersive x-ray spectroscopy (EDS). Microstructural changes in the joint region were examined for a bonding temperature of 560 °C with five different holding time (20 min, 1 h, 2 h, 3 h, and 6 h) under two different applied pressure (0.1 and 0.2 MPa). Kinetics of the bonding process was significantly accelerated in presence of reinforcement (SiC). This acceleration is attributed to the increased solute diffusivity through defects as well as decreased incubation time required for nucleation (SiC particles acting as nucleating agent).

Keywords AlMMC, isothermal solidification, process kinetics, TLPD bonding

1. Introduction

Silicon carbide (SiC) reinforced aluminum-based metal matrix composites (AlMMC) show better properties as compared to monolithic aluminum alloys, which make these composites useful for aerospace and transportation industry applications (Ref 1, 2). However, the difficulty encountered in their joining poses a major problem in widespread industrial applications (Ref 3). Mechanical fastening (bolting or riveting), fusion welding, and solid-state diffusion bonding of such composites involve several difficulties (Ref 4-11) such as damage of reinforcement (for mechanical fastening); formation of brittle phase (Al_4C_3), HAZ cracking & weld porosity (for fusion welding); and excessive plastic deformation under high applied pressure (for solid-state diffusion bonding).

Transient liquid phase diffusion (TLPD) bonding process, which employs an 'interlayer' (often a pure metal) for the formation of low melting point composition (e.g., eutectic), has the advantage of low bonding temperature, low bonding pressure, and less surface finish requirement over solid-state diffusion bonding. However, completion of the TLPD bonding process requires a long time mainly due to prolong isothermal solidification stage. If isothermal solidification is not completed, residual liquid in the interlayer may solidify as brittle phases impairing bond strength (Ref 12). For commercial application of this technique, understanding the microstructural variation at the bond region in order to improve bond strength as well as kinetics of the TLPD process particularly during isothermal solidification is of great importance.

Although a number of investigations have been carried out on TLPD bonding of different metals and alloys, reports on the TLPD bonding of AlMMCs are limited (Ref 9, 13-15). Furthermore, among different interlayer used in TLPD bonding of monolithic aluminum-based alloys, the use of copper interlayer has proved to be successful for joining conventional aluminum alloys and bond strength comparable to that of the parent material has been reported (Ref 16). Again, the published literature on TLPD bonding of AlMMCs mainly dealt with the development of bonding conditions using different thickness of copper interlayer in order to achieve adequate bond strength. For example, Shirzadi and Wallach (Ref 9) achieved a bond strength of 359 Al/SiC (20 wt.% SiC) composite as high as 92% of the parent material strength in low pressure (0.1-0.2 MPa) TLPD bonding using a 7-µm-thick copper interlayer in vacuum followed by isostatic pressing. While studying TLPD bonding of SiC fiber reinforced AlMMC with 10-µm-thick copper interlayer at 550 °C in air environment, Bushby and Scott (Ref 14) reported that higher bonding pressure (20 MPa) was necessary in order to limit oxidation of copper and maximize the bonded area to 80%. However, in these investigations of TLPD bonding of AlMMC no explicit correlation was made between bond microstructure and different stages of the process. In these investigations, applied bonding time is also kept low (maximum 2 h) without any correlation with the completion of isothermal solidification or homogenization of bond region. Also, no comparison of process kinetics is made with monolithic system.

It is reported (Ref 17) that unlike monolithic alloy, AlMMC reinforced with ceramic particles exhibits a high dislocation density and defect-rich particle/matrix interface that accelerates diffusion-assisted process like precipitation hardening. Since TLPD bonding is diffusion controlled process, the presence of SiC particle is expected to accelerate the bonding process of AlMMC. The purpose of the present work is to characterize the

Joydeep Maity, Department of Metallurgical and Materials Engineering, National Institute of Technology, Durgapur, Durgapur 713209, India; **Tapan K. Pal**, Department of Metallurgical and Material Engineering, Welding Technology Center, Jadavpur University, Kolkata 700032, India; and **Rabindranath Maiti**, Central Research Facility, Indian Institute of Technology, Kharagpur 721302, India. Contact e-mail: joydeep_maity@yahoo.co.in.

microstructure of TLPD bonded AlMMC with respect to process kinetics and mechanism in comparison with the reported process kinetics and mechanism in monolithic system.

2. Experimental Procedure

2.1 Material

As-received material for TLPD bonding was an extruded rod of AlMMC consisting of 6061 matrix alloy and 15 wt.% (12.93 vol.%) silicon carbide (SiC) particulate reinforcement. The material was supplied by Regional Research Laboratory, Thiruvanantapuram, India, in the form of cast billet with 23 μm average size of SiC particles. The cast billet was then extruded at National Metallurgical Laboratory, Jamshedpur, India, into a rod at 415 °C temperature with an extrusion ratio 20:1. The nominal composition of 6061 alloy (Ref 18) is given in Table 1. In addition it contains some iron (0.6 wt.%) as an impurity, which was confirmed by optical emission spectroscopy. The density of this as-received extruded AlMMC was also measured by water displacement method.

2.2 Specimen Preparation for Bonding

The extruded rod was machined to produce discs of 15 mm diameter and 10 mm height. As a result the faying surfaces of discs became perpendicular to the extrusion direction. The faying surfaces of discs were polished to 1 μm finish. Pure copper (99.97 wt.%) foil of 50 μm thickness was used as interlayer. The interlayer was punched out to a diameter of 15 mm for bonding. The interlayer and polished faying surfaces of discs were finally rinsed in acetone and dried by a hot air blast just before bonding.

2.3 TLPD Bonding

The interlayer was placed between the polished faying surfaces of the two AlMMC discs. This assembly was then set by an adhesive tape and inserted inside the diffusion bonding unit. The bonding was carried out in a programmable electric furnace keeping bond centerline horizontal. A thermocouple inserted into the drilled hole in one of each pair of discs was used to monitor bonding temperature. The argon gas was flown into the bonding chamber at a rate 5 L/min to maintain inert atmosphere. The bonding temperature was kept at 560 °C, which is above the eutectic temperature (548 °C) of Al-Cu system (Ref 19) and below the solidus temperature (582 °C) of 6061 matrix alloy (Ref 18). The specimens were heated to the bonding temperature (560 °C) at a rate of 6 °C/min, held at that temperature for five different lengths of time (bonding time) viz. 20 min, 1 h, 2 h, 3 h, and 6 h and cooled down to a temperature of 540 °C inside the furnace. Then the specimens were taken out of the furnace and cooled in still air at room temperature. Two different pressures, 0.1 and 0.2 MPa, were applied for bonding.

Table 1 Chemical composition of 6061 alloy (wt.%)

Mg	Si	Cu	Cr	Al
1.0	0.6	0.3	0.2	rest

2.4 Optical Metallography

Bonded cylindrical samples were sectioned perpendicular to the bonding plane using a low speed diamond cutter. The section was polished to 1 μm finish and etched with Kellers reagent (2.5% HNO_3, 1.5% HCl, 0.5% HF, and balance H_2O). Both qualitative and quantitative study of microstructure around bond interface was carried out using optical microscope with digital photomicrography and image analysis facility (ZEISS, Imager.A1m; Dewinter, MICROCAM 5.01). Interface width, grain size (ASTM grain size number), and SiC particle size were measured. Interface width was measured at 'periphery' and 'central zone' of the bond interface. The bond centerline had 15 mm length. The two edges of bond centerline, with each edge of 3.5 mm length, were considered as 'periphery'. The remaining part at the middle of 8 mm length was considered as 'central zone'. The size of SiC particle was considered as an average of major axis and minor axis approximating the particle shape to be an ellipse in two dimension.

2.5 SEM and EDS Analysis

As-polished section was examined around bond interface under scanning electron microscope (JEOL, JSM-5800). Microstructures were studied with both backscattered electron image mode and secondary electron image mode. Reasonable phase contrast was achieved in backscattered electron image mode. Accordingly different phases were identified by EDS spot analysis. Also the progress of diffusion was studied by line scan. The line scan for concentration variation of copper was carried out along a line of 600 μm length lying perpendicular to the bond interface keeping bond centerline approximately at the middle.

3. Results and Discussion

The microstructure of as-received extruded AlMMC as shown in Fig. 1 clearly reveals bands of SiC-rich areas along the extrusion direction as well as some porosity near the particle cluster (band). The presence of porosity is also indicated in the measured density of the composite (2.72 g/cm^3) that shows lower value than the theoretical density of composite (2.77 g/cm^3) based on the calculation from the reported density (Ref 18, 20) of 6061 matrix alloy (2.70 g/cm^3) and SiC (3.21 g/cm^3). The presence of bright $FeAl_3$ intermetallic phase (containing about 61 wt.% Al) is confirmed by SEM backscattered image (Fig. 1c) and EDS Spot analysis. Chemical analysis by optical emission spectrometer indicates the presence of about 0.6 wt.% iron impurity in the composite. The presence of iron impurity (about 0.7 wt.% Fe) in 6061 alloy was reported (Ref 21). Also, the report on the presence of $FeAl_3$ in AlMMC containing iron impurity was published (Ref 14). The formation of $FeAl_3$ phase even for iron content less than 0.6 wt.% is not unexpected since iron has got very little solubility in aluminum as confirmed from Fe-Al phase diagram (Ref 19).

Optical microstructures of TLPD bonded specimens in etched condition representing the bond interface in central zone is shown in Figs. 2 and 3. SEM backscattered images of the bond interface are presented in Figs. 4 and 5. The specimens with minimum bonding time (20 min) exhibit isothermally

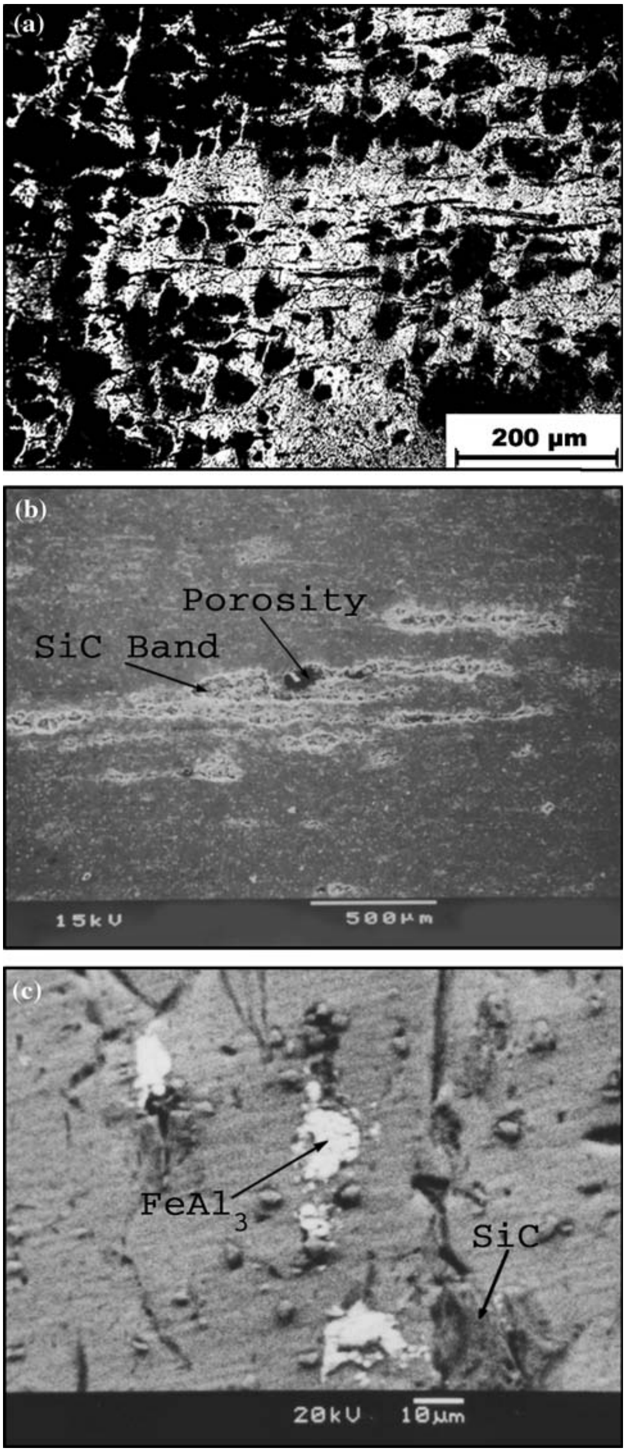

Fig. 1 Microstructure of as-received extruded 6061-SiCp composite. (a) Optical image: bands of SiC along extrusion direction. (b) SEM secondary electron image: SiC bands and porosity. (c) SEM backscattered image: presence of $FeAl_3$

solidified grains (mainly of primary α) adjacent to bond interface (Figs. 2a and 3a). Furthermore, the presence of $CuAl_2$ phase (containing about 54 wt.% Cu) is observed (Fig. 4) adjacent to the bond interface. It is to be noted that as-received AlMMC (unbonded) does not contain any $CuAl_2$ intermetallic phase. This observation indicates that isothermal solidification started before 20 min of bonding time and $CuAl_2$ phase is likely to precipitate out in isothermally solidified zone during cooling from bonding temperature as solubility of Cu in primary α decreases with decreasing temperature following solvus curve.

Based on the study of monolithic system, the TLPD bonding process was described as consisting of four stages by previous investigators (Ref 12, 22, 23), namely, (I) dissolution of interlayer, (II) homogenization of liquid (widening of liquid to its maximum width), (III) isothermal solidification, and (IV) homogenization of bond region. Liu et al. (Ref 24) outlined an analytical model that accounts for the fact that the dissolution front proceeds into the interlayer as well as the parent metal. Using Liu et al's equations the time for complete dissolution of the interlayer is of the order of seconds, as was also calculated by Tuah-Poku et al. (Ref 23). However, analytical models have not been developed to fully describe the widening process of liquid (stage II) and, in fact, there is no discrete boundary in time between stages I and II. Once the interlayer is dissolved, the width of the liquid zone becomes greater than the initial interlayer width. Hence the process of widening occurs concurrently with dissolution. Nakao et al. (Ref 25) and Tuah-Poku (Ref 23) reported that the time required for the liquid widening process (stage II) is of the order of minutes. In present study, heating from eutectic temperature (548 °C) to the bonding temperature (560 °C) at a rate 6 °C/min takes 2 min. It is possible that the first two stages (dissolution of interlayer and widening of liquid) are completed during heating to the bonding temperature. Therefore, liquid widening process completes and isothermal solidification starts before 20 min of holding.

The presence of 15 wt.% SiC particle in 6061 aluminum matrix is expected to have significant effect on TLPD bonding process as compared to pure monolithic system. Microstructural study reveals the segregation of SiC particles at bond centerline with isothermally solidified zones on both sides. During bonding the bond centerline was kept horizontal. Since no preferential segregation occurs toward the lower AlMMC disc, this is not the case of gravity segregation. According to published literature (Ref 26) on general solidification characteristic of SiC reinforced AlMMC, the primary α is very efficient at rejecting SiC, and pushing the particles ahead of the solid/liquid interface. In this regard a critical velocity (V_c) of solid/liquid interface has been reported (Ref 21), below which the SiC particles are pushed by the moving interface and above which they are engulfed. Since the first two stages of TLPD bonding (dissolution of interlayer and widening of liquid) are very fast, the velocity of solid/liquid interface is also very high. As a result SiC particles are not pushed by the solid/liquid interface away from the bond centerline during widening of liquid. The next stage, isothermal solidification, is slow due to solid-state diffusion controlling the process and takes several hours for completion. During isothermal solidification due to low velocity of solid/liquid interface, most of the SiC particles are pushed by the moving solid/liquid interface, as evident in the present work. As a result, particles segregate at bond centerline along with liquid phase and the residual liquid gets solidified during cooling. This aggregate of residual liquid and segregated SiC particles may be called as 'segregation zone' and the width of this segregation zone may be termed as 'interface width'. This is schematically shown in Fig. 6. The measured interface width at central zone and at periphery of bond interface is presented in Table 2. At 20 min bonding time

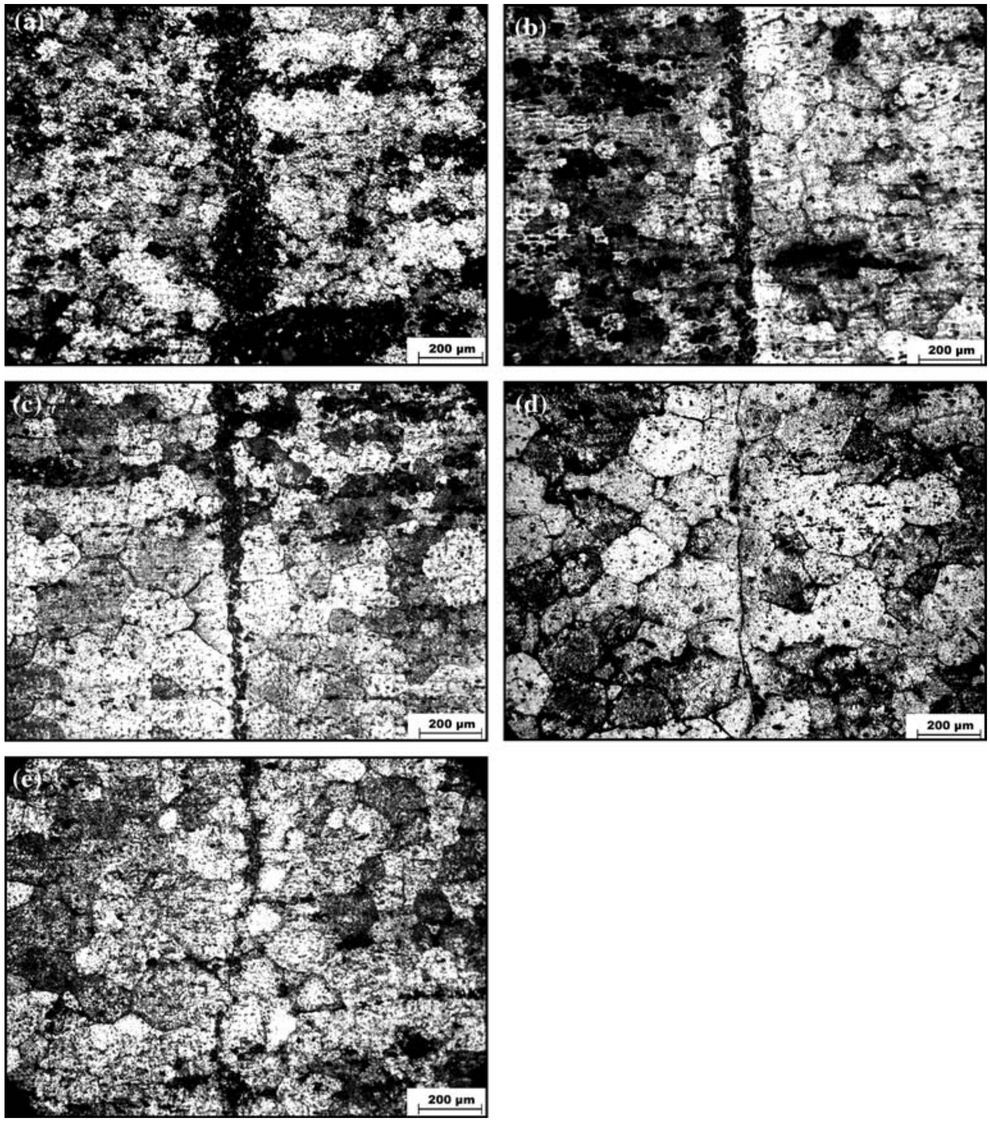

Fig. 2 Optical microstructures of bonded specimens at central zone of bond interface at 0.1 MPa pressure. (a) 20 min, (b) 1 h, (c) 2 h, (d) 3 h, and (e) 6 h

the interface width at central zone is somewhat similar (slightly greater) to that at periphery. However, with increasing bonding time interface width at central zone decreases continuously and always remains lower than that at periphery. This phenomenon indicates that during TLPD bonding under pressure (0.1 and 0.2 MPa) liquid-particle aggregate at interface moves toward periphery and flows out. The evidence of leak out of liquid-particle mixture has been observed. The interface width at periphery exhibits decrease and occasional increase depending on the flow of liquid-particle aggregate from center to periphery and from periphery to outside. Prolong holding (6 h bonding time) reduces the interface width at periphery to the greatest extent (143 μm under 0.1 MPa and 134 μm under 0.2 MPa). Also, with increasing bonding time reduction of interface width at central zone is more at higher pressure (0.2 MPa) than at lower pressure (0.1 MPa). This again indicates more mass flow toward periphery under higher pressure. It is important to note that specimens with 3 and 6 h bonding time (for both the pressures 0.1 and 0.2 MPa) exhibit negligible interface width at central zone with least segregation of SiC particles as shown in Figs. 2d, 2e, 3d, and 3e. Furthermore, the bond interface is hardly discernible and grain continuity exists across the interface indicating the completion of isothermal solidification in 3 h of bonding time. The EDS spot analysis at bond interface of the specimen with 3 h bonding time and 0.2 MPa pressure exhibits the presence of 2.11 wt.% Cu. According to Al-Cu phase diagram (Ref 19), at bonding temperature (560 °C) the maximum solubility of copper in primary α is 4.35 wt.%. Therefore, the copper content of 2.11 wt.% indicates the presence of primary α grains. This further confirms the completion of isothermal solidification.

Microstructural study also reveals that during isothermal solidification, when the solid/liquid interface unidirectionally moves toward bond centerline, few SiC particles are not pushed by the solid/liquid interface, rather they get engulfed (Figs. 2, 3, and 7). However, majority SiC particles are pushed by solid/liquid interface and segregated around bond centerline forming 'segregation zone' as discussed earlier. In fact the critical

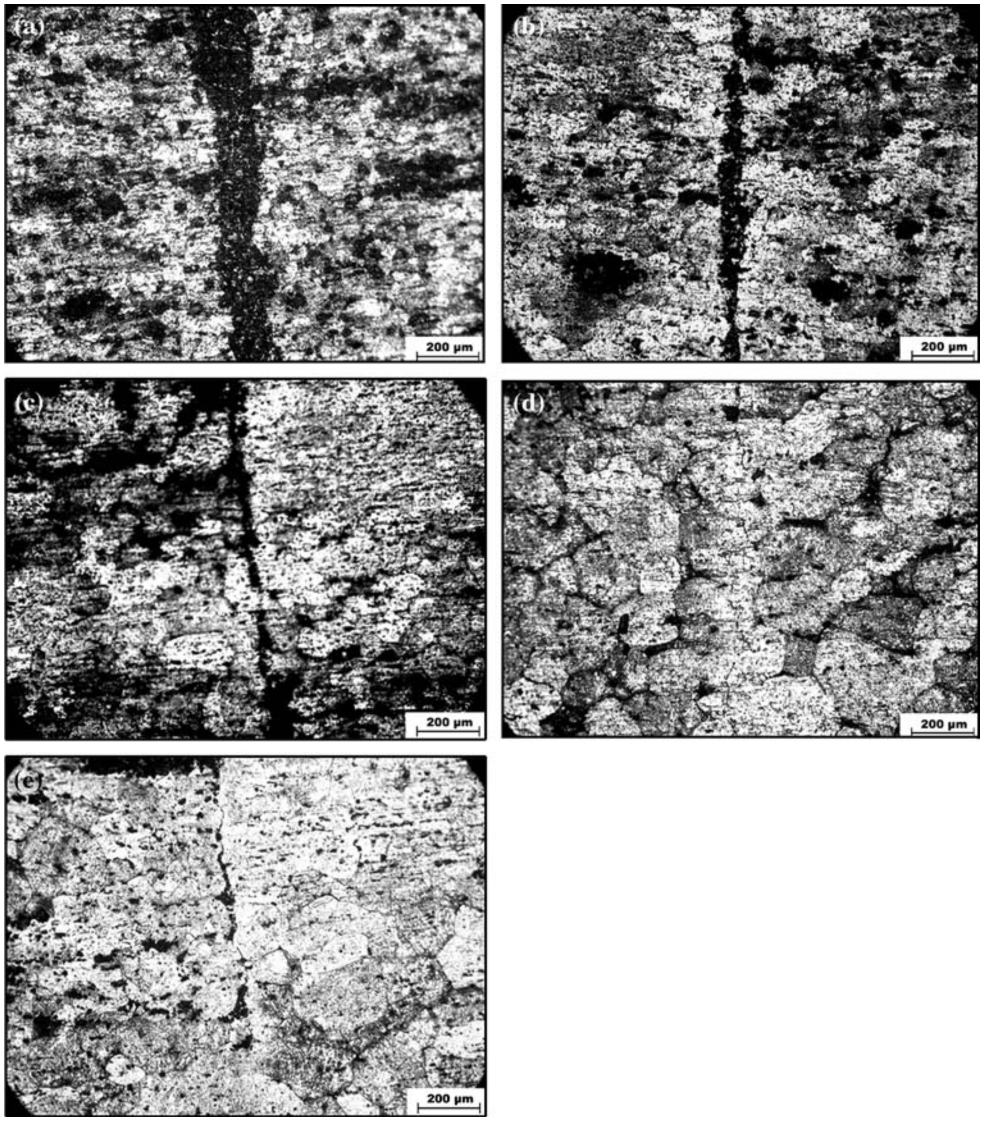

Fig. 3 Optical microstructures of bonded specimens at central zone of bond interface at 0.2 MPa pressure. (a) 20 min, (b) 1 h, (c) 2 h, (d) 3 h, and (e) 6 h

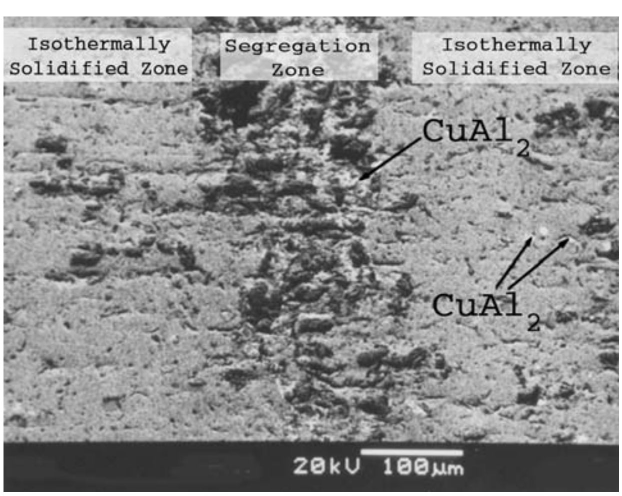

Fig. 4 SEM backscattered image of bonded specimens with lower bonding time (20 min, 0.2 MPa)

velocity depends on several factors including particle size. The critical velocity (V_c) is inversely related to the particle size (Ref 21). Therefore, bigger particle has lower V_c and is likely to be entrapped, whereas smaller particle having higher V_c is likely to be pushed by advancing solid/liquid interface. The size of the SiC particles at 'segregation zone' (containing particles pushed by the solid/liquid interface during isothermal solidification) and at isothermally solidified zone (containing engulfed particles) was measured. The particles in isothermally solidified zone (engulfed particles) are found to be much bigger (size range: 22-30 μm) than the particles in segregation zone (size range: 12-15 μm), as expected. It is also interesting to note that these engulfed SiC particles act as the nucleation sites for isothermal solidification. In isothermally solidified zone, around SiC particles relatively finer grains (ASTM grain size number 6) are observed (Fig. 7). Away from particles the grains are relatively coarser (ASTM grain size number 4) and size of these coarser grains of isothermally solidified zone appears similar to the grains of the base metal. Since the recrystallization temperature range of commercial aluminum alloys is

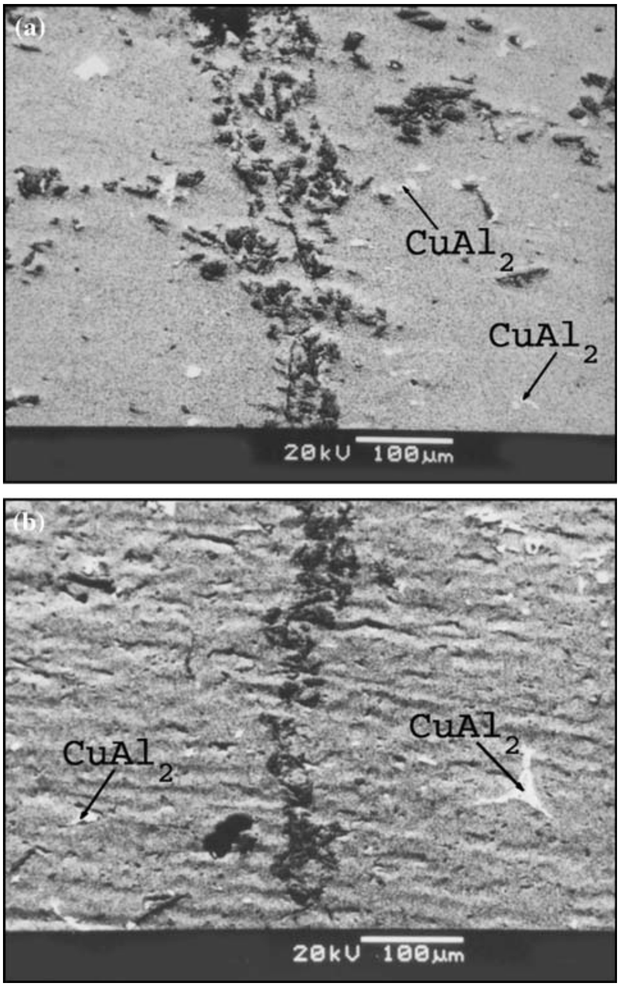

Fig. 5 SEM backscattered image of bonded specimens with higher bonding time. (a) 3 h, 0.1 MPa (near periphery); (b) 3 h, 0.2 MPa (near periphery)

340-410 °C (Ref 27), during extrusion of parent AlMMC at 415 °C fine recrystallized grains (ASTM grain size number 8) appear (Fig. 1a). During bonding at 560 °C these recrystallized grains of base metal as well as isothermally solidified grains grow to larger size.

Rarely any literature deals with joining of AlMMC by TLPD bonding process in relation to its process mechanism. Also, literature on TLPD bonding mechanism specifically for joining pure aluminum or aluminum alloys using Cu interlayer is limited. Natsume et al. (Ref 12) investigated the mechanism of TLPD bonding for joining pure Al by 50 µm Cu interlayer at 570 °C up to a maximum bonding time of 1 h. According to their experimental data, melting of interlayer took about 15 s. Liquid widened to its maximum width of 460 µm ($W_{\max}$) in 60 s. Specimen was not held at bonding temperature till the completion of isothermal solidification. Up to 1 h of maximum holding, liquid width decreased to 406 µm through isothermal solidification. Whereas in the present investigation, in 1 h of bonding time the interface width at central zone has reduced to 107 µm for 0.1 MPa pressure and 86 µm for 0.2 MPa pressure. This indicates much faster kinetics of isothermal solidification for AlMMC than the pure monolithic system. However,

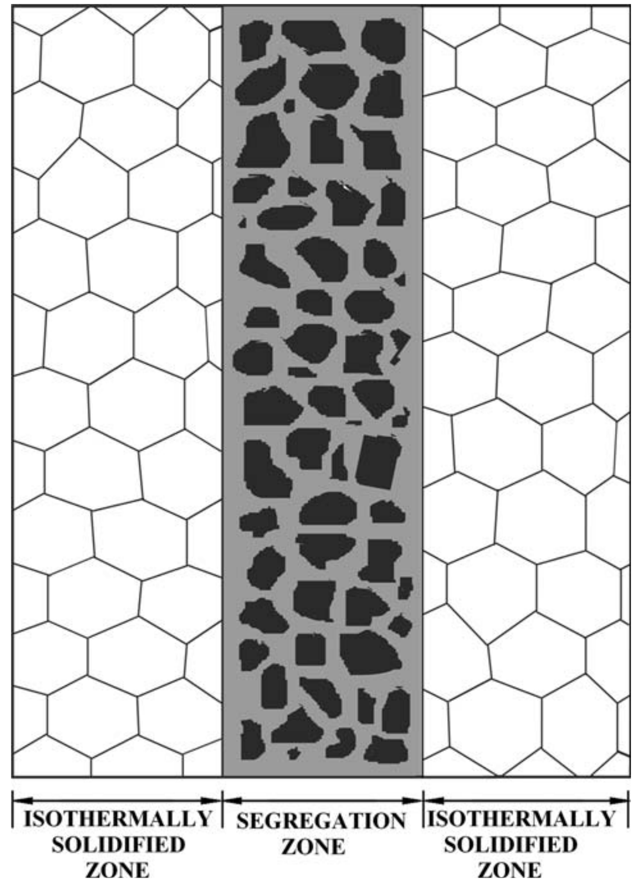

Fig. 6 Schematic representation of bond region during isothermal solidification

Natsume et al. did not continue experimentation till the completion of isothermal solidification. Therefore, the total duration of isothermal solidification for joining aluminum (pure monolithic system) cannot not be obtained directly from their experimental data. On the other hand, Tuah-Poku et al. (Ref 23) fundamentally dealt with TLPD bonding process for monolithic systems and developed analytical rate expressions for different stages of bonding. They developed the following equation for isothermal solidification stage:

$$\log y = c + m \log t \qquad \text{(Eq 1)}$$

where y is the displacement of solid/liquid interface during a time of isothermal solidification t, c and m are constants. Obviously, $y = (W_{\max} - W)/2$, where W is the total width of the liquid in time t and $W_{\max}$ is the maximum liquid width. Fitting the experimental data for isothermal solidification as reported by Natsume et al. to Eq 1, the following equation originates:

$$\log y = 1.0362 \log t - 2.3488 \qquad \text{(Eq 2)}$$

Putting $y = W_{\max}/2$, that is, 230 µm in Eq 2, the duration of isothermal solidification is found out to be 35,153 s (about 9 h 46 min). Therefore, for joining pure Al by 50 µm Cu interlayer at a bonding temperature of 570 °C, isothermal solidification takes about 9 h 46 min for completion. However, in the present study for joining 6061-15 wt.% SiCp by 50 µm Cu interlayer at 560 °C with applied pressure, the completion of isothermal

Table 2 Interface width at central zone and periphery

Bonding pressure	Bonding time	Interface width, μm (mean ± standard deviation) at central zone	at periphery
0.1 MPa	20 min	230 ± 15	185 ± 10
	1 h	107 ± 8	177 ± 17
	2 h	93 ± 11	183 ± 16
	3 h	Negligible	163 ± 18
	6 h	Negligible	143 ± 15
0.2 MPa	20 min	223 ± 17	205 ± 18
	1 h	86 ± 10	173 ± 14
	2 h	73 ± 8	171 ± 15
	3 h	Negligible	196 ± 17
	6 h	Negligible	134 ± 11

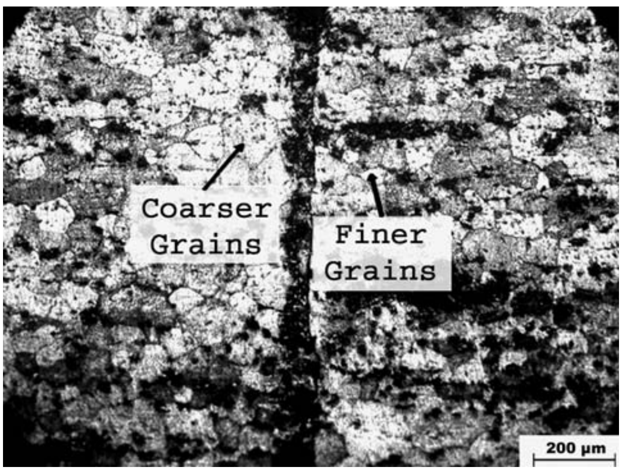

Fig. 7 SiC particles acting as nucleation site for isothermal solidification (0.2 MPa, 1 h)

solidification takes much lesser time (3 h). This is attributed to three major factors. Firstly, in the present study AlMMC contains substantial amount (15 wt.%) of SiC particles. The presence of SiC particles in the metallic matrix leads to the formation of defect-rich interfacial region of high dislocation density, mainly due to the difference in coefficient of thermal expansion between metallic matrix and SiC particles (Ref 17, 28-31). Coefficient of thermal expansion of 6061 matrix alloy and SiC particle are 23.6×10^{-6}/K and 5.5×10^{-6}/K, respectively (Ref 18, 20). Therefore, it is likely that the particle/matrix interface is largely responsible for accelerated diffusion of solute into the base metal. In addition, as discussed earlier, the composite contains some porosity. As a result, diffusion becomes much faster (short circuit diffusion) since the activation energy for short circuit diffusion is considerably smaller than that for lattice diffusion (Ref 32). Secondly, due to application of pressure some part of liquid flows out of periphery, reducing the amount of liquid to be solidified isothermally. Thirdly, as discussed earlier, some SiC particles act as nucleation site to accentuate isothermal solidification process.

The result of line scan shows an occasional rise in copper concentration due to the presence of copper-enriched phase $CuAl_2$. However, on a gross scale, distribution of copper in the matrix for 6 h of bonding is found to be uniform across the bond centerline. This indicates homogenization of bond region. The $CuAl_2$ phase is found to be present at bond interface (segregation zone) as well as in isothermally solidified zone. At

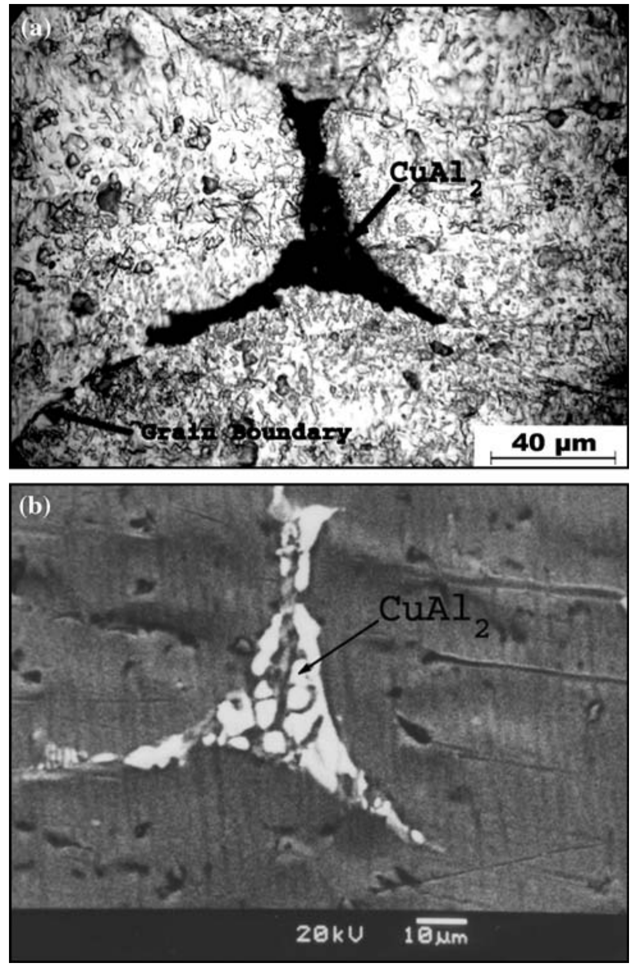

Fig. 8 $CuAl_2$ precipitation at grain boundary in isothermally solidified zone for the TLPD after 3 h, 0.2 MPa. (a) Optical image, (b) SEM backscattered image

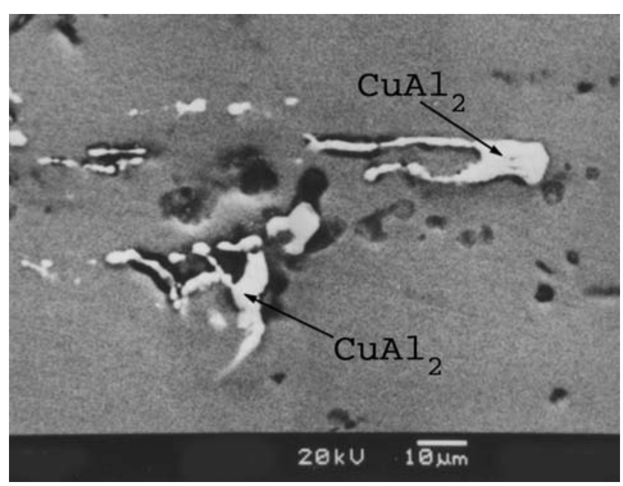

Fig. 9 $CuAl_2$ precipitation at microvoids in isothermally solidified zone (6 h, 0.2 MPa)

the bond interface $CuAl_2$ forms through eutectic solidification of residual liquid during cooling. At the bonding temperature this residual liquid remains intermixed with segregated SiC particles. SEM backscattered image (Fig. 4) clearly reveals that during cooling $CuAl_2$ preferentially nucleates on SiC particles at bond interface. The lower the bonding time, the more $CuAl_2$ phase is present at the bond interface than in isothermally solidified zone. As bonding time increases further, the diffusion of Cu away from the bond interface gradually ceases $CuAl_2$ formation at interface. For higher bonding time (Fig. 5) $CuAl_2$ phase is mostly found to appear in the isothermally solidified zone away from the interface. Isothermally solidified zone contains the grains of primary α. During cooling from bonding temperature, as the solubility of Cu decreases, $CuAl_2$ precipitates out of primary α at high-energy sites such as grain boundary or microvoids. Optical and SEM backscattered image of a typical three armed $CuAl_2$ precipitate at the junction of three grain boundaries present in the isothermally solidified zone is shown in Fig. 8. This precipitate is found to be present at a distance of 250 µm from the bond interface. It is important to note that, in the present investigation, the $CuAl_2$ phase is found to be present up to a maximum distance of 280 µm on each side of the bond centerline. Therefore, the width of the total affected zone in TLPD bonding is about 560 µm. Figure 9 represents the precipitation of $CuAl_2$ at microvoids in the

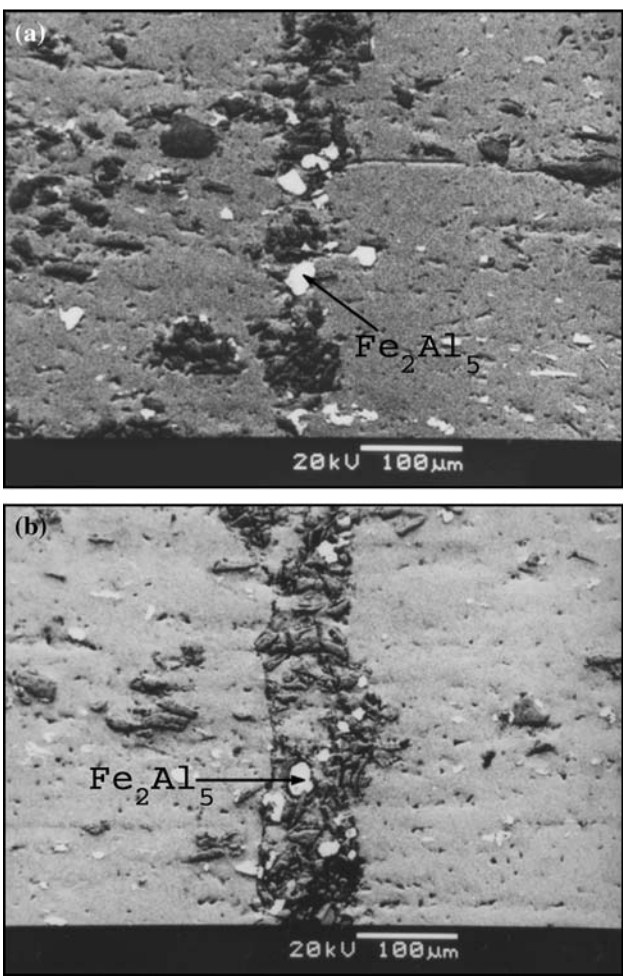

Fig. 10 Segregation of Fe_2Al_5 at bond interface. (a) 1 h, 0.2 MPa (near central zone); (b) 6 h, 0.2 MPa (near periphery)

isothermally solidified zone. The pebble-shaped intermetallic phase (Fe_2Al_5, containing 56 wt.% Al) of iron impurity is found to be segregated mainly at bond interface (Fig. 10). It is likely that during isothermal solidification Fe_2Al_5 particles are pushed by solid/liquid interface and thereby segregate at bond interface (segregation zone) along with SiC particles. The high melting point of Fe_2Al_5 (1169 °C) and the stability of Fe_2Al_5 phase around bonding temperature (560 °C) as obtained from the phase diagrams of binary Fe-Al and ternary Al-Cu-Fe systems (Ref 19, 33) further confirm this possibility.

4. Conclusion

(1) The TLPD bonding process of 6061-SiCp composite occurs much faster than that of pure aluminum. Isothermal solidification takes only 3 h, which is about one-third the time taken in pure system. Bond region gets homogenized in 6 h.
(2) The engulfed SiC particles acting as nucleation site accelerate isothermal solidification. During isothermal solidification majority SiC particles are not engulfed and are pushed by the moving solid/liquid interface. These particles segregate at the bond interface along with residual liquid. Simultaneously, under applied pressure the mass of residual liquid and segregated SiC particles at bond interface gradually moves toward periphery and ultimately flows out with increasing bonding time. This reduces the amount of residual liquid to be solidified, thereby shortening the duration of isothermal solidification.
(3) The $CuAl_2$ phase is found to be present at the bond interface (segregation zone) as well as in isothermally solidified zone. At the bond interface $CuAl_2$ forms through eutectic solidification of residual liquid during cooling and it preferentially nucleates on segregated SiC particles. The lower the bonding time, the more is the proportion of $CuAl_2$ phase present at the bond interface.
(4) As bonding time increases further, the diffusion of Cu away from the interface gradually ceases $CuAl_2$ formation at the bond interface and the $CuAl_2$ phase is mostly found to appear in the isothermally solidified zone away from the interface in the form of precipitate at high-energy sites (grain boundary, microvoids, etc.).
(5) Pebble-shaped Fe_2Al_5 phase of iron impurity segregates mainly at the bond interface.

References

1. D. Huda, M.A. El baradie, and M.S.J. Hashmi, Meta-Matrix Compsites: Materials Aspects, Part II, *J. Mater. Process. Technol.*, 1993, **37**(1–4), p 529 –541
2. T.J. Lienert, W.A. Baeslack, J. Ringnalda, and H.L. Fraser, Inertia-Friction Welding of SiC-Reinforced 8009-Aluminium, *J. Mater. Sci.*, 1996, **31**(8), p 2149 –2157
3. M.B.D. Ellis, Joining of Metal Matrix Composites—A Review, *TWI J.*, 1997, **6**(1), p 69–128
4. W.I. Hall and F. Manrique, Surface Treatment of Carbon Fiber for Aluminium Alloy Matrix Composites, *Scr. Met.*, 1995, **33**(12), p 2037–2043
5. M.F. Gittos and P.L. Threadgill, Preliminary Studies of Joining Particulate Reinforced Aluminium Alloy Metal Matrix Composites, *Metal Matrix Composites III: Exploiting the Investment*, Inst. of Metals, December 10–11, 1991

6. T.S. Luhman, R.L. Williams, and K.B. Das, *Development of Joint and Joining Techniques for Metal Matrix Composites*, Fourth Quarterly Progress Report, Army Materials and Mechanics Research Center, 1983, p 1–58
7. J.H. Devletian, *SiC/Al Metal Matrix Composite Welding by a Capacitor Discharge Process*, AWS 68th Annual Meeting, Welding Journal, Chicago, IL, 1987, **66**, p 33–39
8. R.S. Bushby and V.D. Scott, Liquid Phase Bonding of Aluminium and Aluminium/Nicalon Composite Using Interlayers of Cu-Ag Alloy, *Mater. Sci. Technol.*, 1995, **11**(7), p 643–649
9. A.A. Shirzadi and E.R. Wallach, New Approaches for Transient Liquid Phase Diffusion Bonding of Aluminium Based Metal Matrix Composites, *Mater. Sci. Technol.*, 1997, **13**(2), p 135–142
10. D.J. Field, Aluminium Alloys—Contemporary Research and Applications, *Lond Acad Press*, 1989, **31**, p 523–537
11. A. Urena, J.M. Gomez De Salazar, and M.D. Escalera, *Key Eng. Mater.*, 1995, p 104–107, 523–540
12. Y. Natsume, K. Ohsasa, Y. Tayu, T. Momono, and T. Narita, Numerical Modeling of Transient Liquid-Phase Diffusion Bonding Process of Al using Cu Filler Metal, *ISIJ Int.*, 2003, **43**(12), p 1976–1982
13. P.G. Partridg and D.V. Dunford, *J. Mater. Sci.*, 1991, **26**, p 2255–2258
14. R.S. Bushby and V.D. Scott, Liquid Phase Bonding of Aluminium and Aluminium/Nicalon Composite Using Copper Interlayers, *Mater. Sci. Technol.*, 1993, **9**(5), p 417–423
15. T.K. Pal, Joining of Aluminium Metal Matrix Composites, *Mater. Manuf. Processes*, 2005, **20**, p 717–726
16. A.E. Dray, Diffusion Bonding of Aluminium, PhD thesis, University of Cambridge, 1985
17. J.M. Papazian, Effects of SiC Whiskers and Particles on Precipitation in Aluminium Matrix Composites, *Metall. Trans. A*, 1988, **19A**(12), p 2945–2953
18. Anon, Properties and Selection: Non-ferrous Alloys and Special-Purpose Materials, *Metals Handbook*, 10th edn., ASM International, The Materials Information Society, 1990, **2**, p 102–103
19. Anon, Alloy Phase Diagrams, *ASM Handbook*, ASM International, The Materials Information Society, 1992, **3**, p 2.44–3.10
20. Anon, Ceramics and Glasses, *Engineering Materials Handbook*, ASM International, The Materials Information Society, 1991, **4**, p 30
21. P.K. Rohatgi, R. Asthana, and S. Das, Solidification, Structures, and Properties of Cast Metal-Ceramic Particle Composites, *Int. Met. Rev.*, 1986, **31**(3), p 115–136
22. D.S. Duvall, W.A. Owczarski, and D.F. Paulonis, TLP Bonding: A New Method for Joining Heat Resistant Alloys, *Weld. J.*, 1974, **53**(4), p 203–214
23. I. Tuah-Poku, M. Dollar, and T.B. Massalski, A Study of the Transient Liquid Phase Bonding Process Applied to a Ag/Cu/Ag Sandwich Joint, *Metall. Trans. A*, 1988, **19A**(3), p 675–686
24. S. Liu, D.L. Olson, G.P. Martin, and G.R. Edwards, *Weld. J.*, 1991, **70**, p 207–215
25. Y. Nakao, K. Nishimoto, K. Shinozaki, and C. Kang, Theoretical Research on Transient Liquid Insert Metal Diffusion Bonding of Nickel Base Alloys, *Trans. Jpn. Welding Soc.*, 1989, **20**(1), p 60–65
26. M. Gallerneault, M. Kaya, R.W. Smith, and G.W. Dellamore, Ultimate Sediment Concentration in Directionally Solidified Al-Si/SiC Particulate Metal Matrix Composites, *Proc. Conf. on Extraction, Refining and Fabrication of Light Metals*, Ottawa, Ontario, Canada, August 18–21, 1991, Pergamon Press Inc., New York, p 69–81
27. Aluminium, Properties, Physical Metallurgy & Phase Diagrams, K.R. Van Horn, Ed., American Society of Metals, Ohio, Metals Park, 1967, I, p 98
28. A.R. Champion, W.H. Krueger, H.S. Hartman, and D.K. Dhingra, *Proceedings of the 1978 International Conference on Composite Materials* – ICCM/2 TMS-AIME, New York, 1978, p 883
29. D.J. Lloyd, *Int. Mater. Rev.*, 1994, **39**(1), p 1
30. W.S. Miller and E.J. Humphreys, *Scr. Metall. Mater.*, 1991, **25**, p 33
31. R.J. Arsenault, *Scr. Metall. Mater.*, 1991, **25**, p 2617
32. N.A. Gjostein, Short Circuit Diffusion, in *Diffusion*, Papers Presented at a Seminar of the American Society for Metals, October 14–15, 1972, American Society for Metals, Metals Park, Ohio, p 241
33. Anon, *Ternary Alloys, a Comprehensive Compendium of Evaluated Constitutional Data and Phase Diagrams*, G. Petzow and G. Effenberg, Eds., VCH, Weinheim, 1991, **4**, p 475–489